10-1-2012

Elastic deformations of the rotary double motor of single F(o)F(1)-ATP synthases detected in real time by Förster resonance energy transfer.

Stefan Ernst

Monika G Düser

Nawid Zarrabi

Stanley D Dunn

Michael Börsch

Biochimica et Biophysica Acta 1817 (2012) 1722–1731

Contents lists available at SciVerse ScienceDirect

Biochimica et Biophysica Acta

journal homepage: www.elsevier.com/locate/bbabio

Elastic deformations of the rotary double motor of single F_OF_1-ATP synthases detected in real time by Förster resonance energy transfer ☆

Stefan Ernst [a,b], Monika G. Düser [a], Nawid Zarrabi [a], Stanley D. Dunn [c], Michael Börsch [a,b,*]

[a] 3rd Institute of Physics, University of Stuttgart, Pfaffenwaldring 57, 70550 Stuttgart, Germany
[b] Single-Molecule Microscopy Group, Jena University Hospital, Friedrich Schiller University Jena, Nonnenplan 2-4, 07743 Jena, Germany
[c] Department of Biochemistry, University of Western Ontario, London, Ontario, Canada N6A 5C1

ARTICLE INFO

Article history:
Received 18 January 2012
Received in revised form 25 March 2012
Accepted 29 March 2012
Available online 5 April 2012

Keywords:
F_OF_1-ATP synthase
Rotary motor
Elastic deformation
Förster resonance energy transfer
Single-molecule FRET

ABSTRACT

Elastic conformational changes of the protein backbone are essential for catalytic activities of enzymes. To follow relative movements within the protein, Förster-type resonance energy transfer (FRET) between two specifically attached fluorophores can be applied. FRET provides a precise ruler between 3 and 8 nm with subnanometer resolution. Corresponding submillisecond time resolution is sufficient to identify conformational changes in FRET time trajectories. Analyzing single enzymes circumvents the need for synchronization of various conformations. F_OF_1-ATP synthase is a rotary double motor which catalyzes the synthesis of adenosine triphosphate (ATP). A proton-driven 10-stepped rotary F_O motor in the *Escherichia coli* enzyme is connected to a 3-stepped F_1 motor, where ATP is synthesized. To operate the double motor with a mismatch of step sizes smoothly, elastic deformations within the rotor parts have been proposed by W. Junge and coworkers. Here we extend a single-molecule FRET approach to observe both rotary motors simultaneously in individual F_OF_1-ATP synthases at work. We labeled this enzyme with two fluorophores specifically, that is, on the ε- and *c*-subunits of the two rotors. Alternating laser excitation was used to select the FRET-labeled enzymes. FRET changes indicated associated transient twisting within the rotors of single enzyme molecules during ATP hydrolysis and ATP synthesis. Supported by Monte Carlo simulations of the FRET experiments, these studies reveal that the rotor twisting is greater than 36° and is largely suppressed in the presence of the rotation inhibitor DCCD. This article is part of a Special Issue entitled: 17th European Bioenergetics Conference (EBEC 2012).

1. Introduction

F_OF_1-ATP synthases are the ubiquitous enzymes catalyzing the formation of adenosine triphosphate (ATP) from adenosine diphosphate (ADP) and phosphate. Many details of the molecular mechanism of this enzyme have been unraveled in the last 15 years based on single-molecule detection of conformational changes. Rotation of subunit γ to coordinate the sequential ATP synthesis steps in the three catalytic binding sites in the F_1 part, as proposed by P. Boyer [1] and implied by the crystal structure of the mitochondrial F_1 by J. Walker and coworkers [2], was first demonstrated unequivocally in isolated F_1 by H. Noji and colleagues [3]. They attached a fluorescent marker on the γ-subunit of surface-immobilized F_1 and monitored rotation of the 2-μm-long marker by videomicroscopy during ATP hydrolysis. Reducing the size of the marker using 40 nm gold beads and laser light scattering in dark-field microscopy allowed detection of angular dependencies of different steps of ATP hydrolysis in F_1, that is ATP binding, catalysis, and ADP as well as phosphate release [4–6]. Small magnetic beads attached to the γ-subunit enabled the use of external magnetic fields on individual F_1 molecules to mechanically rotate and stall the γ-subunit [7–9]. Thus, torque and thermodynamic properties of the chemo-mechanical energy conversion from the ATP hydrolysis reaction in the binding pocket to rotary movement of γ could be measured [10]. Similarly, rotation of the ε-subunit of the F_1 part [11–13] and the *c*-ring of the F_O part have been shown during ATP hydrolysis [14–18].

To monitor subunit rotation during ATP synthesis in the complete F_OF_1-ATP synthase reconstituted in a lipid membrane, different approaches have been developed. A sophisticated biochemical assay used F_1 with one radioactively tagged β-subunit and two non-radioactive β-subunits to generate a reversible crosslink with the γ-subunit. These studies provided evidence that γ changes its orientation during rotary catalysis with respect to the tagged β-subunit [19,20] during ATP synthesis. Rotation of the *c*-ring was inferred from single-

☆ This article is part of a Special Issue entitled: 17th European Bioenergetics Conference (EBEC 2012).

* Corresponding author at: Single-Molecule Microscopy Group, Jena University Hospital, Friedrich Schiller University Jena, Nonnenplan 2-4, 07743 Jena, Germany. Tel.: +49 3641 933745; fax: +49 3641 933750.
E-mail addresses: s.ernst@physik.uni-stuttgart.de (S. Ernst), m.dueser@physik.uni-stuttgart.de (M.G. Düser), n.zarrabi@physik.uni-stuttgart.de (N. Zarrabi), sdunn@uwo.ca (S.D. Dunn), michael.boersch@med.uni-jena.de (M. Börsch).

0005-2728/$ – see front matter © 2012 Elsevier B.V. All rights reserved.
doi:10.1016/j.bbabio.2012.03.034

fluorophore anisotropy imaging in the Na^+-driven surface-attached F_OF_1-ATP synthase of *Propionigenium modestum* [21]. Simultaneous crosslinking of all three rotor subunits γ, ε and *c* in *Escherichia coli* F_OF_1-ATP synthase did not affect ATP hydrolysis, ATP synthesis or DCCD inhibition [22] strongly supporting a co-rotation of these subunits.

Alternatively, single-molecule Förster resonance energy transfer (FRET) with two small markers specifically attached to one rotary and one static subunit was applied by the group of P. Gräber [23–26]. FRET allows measurement of distances between two fluorophores in the range of approximately 2 nm to 10 nm with subnanometer precision. The sensitivity of photon detectors is high enough that single FRET-labeled enzymes can be analyzed with submillisecond time resolution for the distance measurements. Accordingly, subunit rotation in appropriately engineered and labeled single F_OF_1-ATP synthase complexes of *E. coli* can be monitored in real time. The basic principle is shown in Fig. 1. By attaching one fluorophore *via* genetically introduced cysteines to an off-axis position on one of the rotary subunits and a second fluorophore to the static subunits on the peripheral stalk (*b*-subunits) or the *a*-subunit of the enzyme, the distance between the two dyes varies within the range of 3 nm to 8 nm during rotation, perfectly matching the maximum sensitive range of FRET. Thereby, rotation of the γ [27,28] and ε-subunits [29,30] in three 120° steps was shown to occur in opposite directions during ATP synthesis and ATP hydrolysis, and upper limits of the transition times between the three catalytic dwells per full rotation were determined [31]. Dwell time analysis revealed differences in the mechanism of Aurovertin B inhibition of ATP synthesis and hydrolysis for the *E. coli* enzyme [32]. With single-molecule FRET, we could show that the *c*-ring in the F_O part rotates in sequential 36° steps during ATP synthesis by *E. coli* F_OF_1-ATP synthase [33].

Different step sizes for the two rotary motors have also been reported for the *Thermus thermophilis* ATP synthase [34,35], reinforcing the fundamental question of how the protein is able to couple motors with distinct stepping characteristics. Elements of elastic deformation in the peripheral stator subunits or within the three rotary subunits have been proposed by W. Junge and others [36–38]. Experimental evidence for elastic protein domains within the rotor as well as a surprisingly high stiffness of the peripheral stalk, that is, the asymmetric right-handed coiled-coil *b*-subunit dimer [39–41]), has been determined using videomicroscopy of the Brownian fluctuations of beads attached to ATP synthase molecules containing engineered disulphide cross-links that allowed measurement of the torsional stiffness of specific parts of the enzyme [10,42–45]. The results of some of these studies also allowed application of a "computational microscope" approach (K. Schulten) by Molecular Dynamics Simulations which provided an atomic-level description of torsional elasticities within the rotor [46].

To identify elastic deformations within the rotor subunits without attachment of large beads and to observe these conformational fluctuations during ATP synthesis, we have recently expanded our single-molecule FRET approach to a three-fluorophore experiment [47,48]. The aim of the advanced and complex spectroscopic set-up was to ensure that internal deformations of the rotor as measured by FRET changes can be correlated with an overall rotation of the three subunits, *i.e.* catalytic activity of the enzyme. Thus, photophysical artifacts on the single-molecule fluorescence level like spectral fluctuations and blinking could be discriminated from a transient twisting of ε- *versus* the *c*-subunits. Indications for relative movements between ε and *c* had been found by P. Gräber and coworkers [49].

Here, we re-use this triple-mutant of *E. coli* F_OF_1-ATP synthase. However, the fluorescent protein EGFP fused to the C-terminus of the *a*-subunit was not used for the FRET measurements. Instead, the ε-subunit labeled with Alexa-532 through a cysteine at residue 56 acted as the FRET donor, and a Cy5 fluorophore on a cysteine introduced at residue 2 on one of the ten *c*-subunits acted as FRET acceptor. Thus, alterations in the FRET efficiency for any particular molecule will be indicative of conformational changes within the rotor. Fig. 1B shows a simplified model for the stopping positions of a *c*-subunit with respect to a fixed position of the ε-subunit, and illustrates the ten possible FRET efficiencies for any given labeled *c*-subunit, respectively. Based on the previous FRET experiments, we quantitatively analyzed the relative movements of ε and *c* during both ATP synthesis and ATP hydrolysis. We found an extensive twisting in this section of the rotor, encompassing the β-barrel domain of ε and the *c*-ring, significantly greater than 36° and possibly in the range of up to 108°, indicating that a substantial fraction of the total rotor torsional elasticity is contained within these domains.

2. Materials and methods

2.1. E. coli F_OF_1-ATP synthase mutant

The triple-mutant enzyme used for the single-molecule FRET experiments was constructed by re-assembling two different mutants

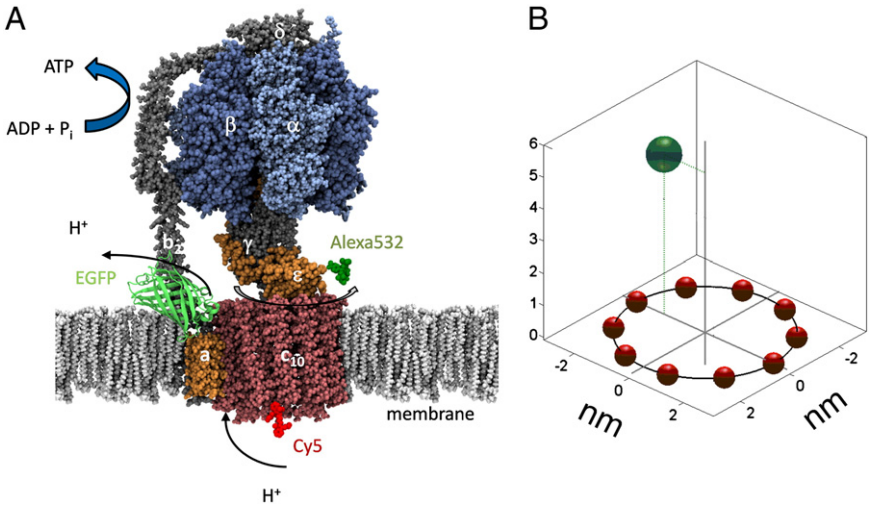

Fig. 1. A, Principle of elastic deformation measurement by single-molecule FRET between the two fluorophores Alexa-532 (green dye molecule) on the ε-subunit of the central stalk and Cy5 (red dye molecule) on one of the ten *c*-subunits on the periplasmic side of the membrane. A triple-mutant of *E. coli* F_OF_1-ATP synthase with EGFP fused to the C-terminus of the *a*-subunit was used [48]. B, Model for the relative distances of the two fluorophores (Alexa-532 on ε corresponds to the green dot; ten possible Cy5 positions on *c* correspond to red dots) with respect to the axis of rotation (gray).

of the *E. coli* F_OF_1-ATP synthase which have been published previously [29,33]. Briefly, the cysteine mutant εH56C in F_1 was produced by plasmid pRAP100 in *E. coli* strain RA1. F_1 was prepared as described [29] and labeled with Alexa-532-maleimide (Invitrogen). The efficiency of labeling was determined by UV–VIS absorbance spectroscopy to be 35%.

A double-mutant F_OF_1-ATP synthase with the autofluorescent protein EGFP fused to the N-terminus of the *a*-subunit and a cysteine introduced to residue position 2 of the *c*-subunits is encoded by plasmid pDC61, which was expressed in strain RA1 for purification of the F_OF_1 holoenzyme as described [33]. After substoichiometric labeling of the *c*-ring of about 7.4% with Cy5-monomaleimide (Amersham CyDye, GE Healthcare Life Sciences) the enzyme was reconstituted into preformed liposomes by a standard detergent/Biobeads procedure [50]. The unlabeled F_1 sector was dissociated from F_O remaining in the membrane in the presence of Mg^{2+}-free buffer, and Alexa-532-labeled F_1 was re-assembled to the F_O sector in liposomes to yield functional F_OF_1-ATP synthase with FRET donor Alexa-532 and FRET acceptor Cy5. ATP hydrolysis activity was determined to 52 ATP/s at 1 mM ATP, and ATP synthesis activity to 31 ATP/s at room temperature with 100 μM ADP, 5 mM P_i, and an initial pH difference of 4.1 after an acid–base transition in the presence of an initial K^+/valinomycin diffusion potential of 120–140 mV [28]. ATP synthesis rate of wildtype *E. coli* F_OF_1-ATP synthase was 69 ATP/s for the same conditions. Aliquots of 2 μl of the reconstituted FRET-labeled F_OF_1-ATP synthases were shock-frozen in liquid nitrogen and stored at −80 °C until use.

2.2. Confocal single-molecule FRET microscope and data analysis

For the single-molecule FRET measurements we used a custom-designed confocal microscope with piezo-driven three dimensional sample scanning based on an Olympus IX 71 microscope [51–54] (Fig. 2a). Briefly, the beam of a continuous-wave solid state laser (Compass 315 M, Coherent, Lübeck, Germany) with 532 nm emission was overlaid with a picosecond-pulsed laserdiode (LDH-P-635B, Picoquant, Berlin, Germany) with 635 nm emission (30 μW) by a dichroic beam combiner (DCXR 540, AHF Analysentechnik, Tübingen, Germany). Both lasers were operated in alternating laser excitation (ALEX, [55]) mode by switching the 532 nm laser with an acousto-optical modulater (AOM, model 3350-192, Crystal Technologies). AOM and pulsed laser diode were synchronized by an Arbitrary Waveform Generator (AWG 2041 with 8 digital ECL outputs, Tektronix) with 1 ns time resolution [56]. Both laser beams were redirected by a beam splitter (triple-band 488/532/633, AHF Analysentechnik, Tübingen, Germany) and an Olympus water immersion objective (UPlanSApo 60x, 1.2 N.A.) into the same confocal exitation volume of about 10 fl (Fig. 2b). Laser power was 150 μW for 532 nm and 30 μW for 635 nm at the back aperture of the microscope objective.

Two single photon counting avalanche photodiodes (APD) separated by a dichroic filter at 630 nm (DCXR 630, AHF Analysentechnik, Tübingen, Germany) detected the fluorescence in two spectral ranges for the FRET donor intensities (545 nm to 625 nm) and FRET acceptor intensities (663 nm to 737 nm). Recording of photons was achieved by two synchronized counter cards in a computer (two cards of a three-channel TCSPC-153 bundle, Becker&Hickl, Berlin, Germany) yielding two time resolutions for each photon: the microtime in nanoseconds for the photon arrival time with respect to the pulse sequence of ALEX, and the macrotime with respect to the start of the experiment. Macrotime information was used for binning photons in time intervals of 1 ms by our software "Burst_Analyzer" to obtain FRET time trajectories [57].

Microtime information was used to sort the photons detected in the Cy5 fluorescence channel for either FRET acceptor intensities following 532 nm excitation, or for the simultaneous control measurement to check the existence of Cy5 on each F_OF_1-ATP synthase following the 635 nm laser pulse (Fig. 2c). Briefly, alternating laser excitation was synchronized by the AWG using three digital outputs. One output triggered a 60-picosecond pulse at 635 nm to excite only the Cy5 label at F_OF_1-ATP synthase in a time window of 14 ns. The second output triggered the AOM for a 25 ns "on-pulse" of the 532 nm laser delayed by 22 ns with respect to output one. The third output was used to set the sequence window of 64 ns for the synchronized TCSPC photon counter cards. This AWG sequence resulted in a duty cycle for FRET excitation with 532 nm of (25 ns/64 ns) = 39% for DCO-ALEX.

To identify photon bursts of freely diffusing, reconstituted, FRET-labeled F_OF_1-ATP synthases in liposomes, we applied an automatic search algorithm (implemented in the "Burst_Analyzer" software) on the FRET time trajectories by intensity threshold criteria after background correction of 2 counts/ms in FRET donor channel and 1 count/ms in the FRET acceptor channel. Here, a minimal rates of 10 counts/ms in the FRET donor as well as 10 counts in the FRET acceptor channel were set. Simultaneously, also a minimal rate of 8 counts/ms was set in the Cy5 control channel (635 nm excitation for "acceptor test"). Once these thresholds were achieved for a photon burst, the beginning and end of the burst were set at flank intensity levels of 5 counts/ms or 4 counts/ms, for the FRET and control channels, respectively. Then, photon bursts with minimal duration of 20 ms and maximal duration of 200 ms were stored for further analysis. Within a defined photon burst, a maximum time of 2 ms was allowed for the three flank intensity thresholds to fall below the set points. Afterwards each photon burst was inspected manually

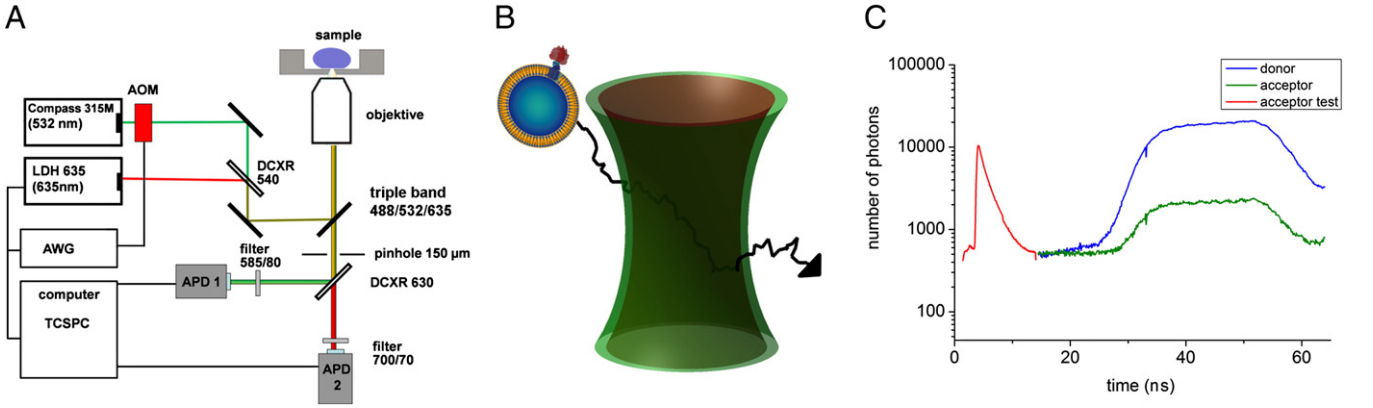

Fig. 2. Setup of the confocal microscope used for FRET detection of rotor elasticities in single reconstituted F_OF_1-ATP synthases. A, Alternating laser excitation triggered by an Arbitrary Waveform generator and fluorescence pathway with interference filters. B, Principle of confocal single-molecule FRET with freely diffusing proteoliposomes. C, Sorting of photons according to the excitation laser pulse into FRET donor photons (blue curve in the microtime histogram, Alexa-532), FRET acceptor photons (green curve, Cy5) and directly excited Cy5 (red curve).

and FRET efficiency levels were assigned according to fluctuations of the calculated fluorophore distance trajectory [58]. FRET efficiency levels were added to histograms and plotted using our software tools written in Matlab (Mathworks, Inc.). For the distance calculation from FRET efficiencies according to Förster theory [59], we used the fluorescence quantum yields (Alexa-532 $\phi = 0.61$; Cy5 $\phi = 0.28$; Förster radius $R_0 = 5.3$ nm), cross talk correction for Alexa-532 fluorescence in the Cy5 detection channel (2.5%) and corrected detection efficiencies d of the two spectral ranges for the microscope setup (Alexa-532 $d = 0.22$; cy5 $d = 0.36$; resulting correction factor $\gamma = 0.77$). Fluorescence anisotropies of FRET donor as well as FRET acceptor bound to single F_OF_1-ATP synthases reconstituted to liposomes had been previously determined (details to be published elsewhere).

3. Results

3.1. The triple-mutant of F_OF_1-ATP synthase is functional

The functionality of the F_OF_1-ATP synthase mutant was determined after re-assembly of F_1 sectors labeled with Alexa-532 at the ε-subunit (εH56C) to F_O comprising EGFP fused to the C-terminus of the *a*-subunit and Cy5 attached to one *c*-subunit (*c*2C) of the *c*-ring. The reconstituted, triple-labeled enzymes showed ATP hydrolysis rates in the range of 50 ATP/s at room temperature in the presence of 1 mM ATP and 2.5 mM Mg^{2+} which is comparable to the activities measured for the individual mutations in *E. coli* F_OF_1-ATP synthase [29,33]. The labeled enzymes achieved maximal ATP synthesis rates of 31 ATP/s at room temperature in the presence of 100 μM ADP, 5 mM P_i and an initial ΔpH of 4.1 plus electric potential. These rates support the minor effects of the individual mutations as reported previously [29,30,33]. In the presence of DCCD (60 μM) or after addition of the ATP analog AMPPNP (1 mM) to the buffers used for ATP hydrolysis or ATP synthesis measurements, activity of the enzyme was nearly abolished.

3.2. Single-molecule FRET recordings during ATP hydrolysis

For ATP hydrolysis measurements with the confocal microscope, a 2-μl aliquot of reconstituted FRET-labeled F_OF_1-ATP synthase was thawed and diluted 5 times with buffer A (20 mM tricine-NaOH, 20 mM succinic acid, 2.5 mM $MgCl_2$, 0.6 mM KCl) at pH 8.0. Immediately before the single-molecule FRET recording, proteoliposomes were diluted further 1:100 with buffer A which also contained 1 mM ATP. Fig. 3A shows three photon bursts of freely diffusing FRET-labeled F_OF_1-ATP synthases. The three fluorescence intensity trajectories in the lower panels correspond to the FRET donor Alexa-532 (blue trace) and the FRET acceptor Cy5 (green trace) as well as the Cy5 fluorescence (red trace) directly excited with a 635 nm pulse to check that both fluorophores were attached to the same F_OF_1-ATP synthase. The control was necessary since labeling was substoichiometric (see Materials and methods), and only ~10% of all photon bursts of single F_OF_1 with Alexa-532 on ε also contained Cy5 on *c* according to this control with the alternating red laser.

A total number of 556 FRET-labeled F_OF_1-ATP synthases were detected within 300 min of recording (twenty 15-min measurement periods, see Table 1). FRET changes were identified in the corresponding Alexa-532–Cy5 distance trajectories for each photon burst as shown in the upper panels in Fig. 3A. Here we were interested in the largest possible FRET distance change. Therefore, FRET level assignment mostly focussed on the minimum and maximum FRET efficiency found within a single photon burst. For a maximum likelihood-based FRET-to-distance conversion, we have implemented the "FRETtrace" program from G. Schöder and H. Grubmüller [58] into our FRET data analysis software "Burst_Analyzer". The FRET distance trajectories were inspected in each photon burst. Two F_OF_1-ATP synthase molecules in

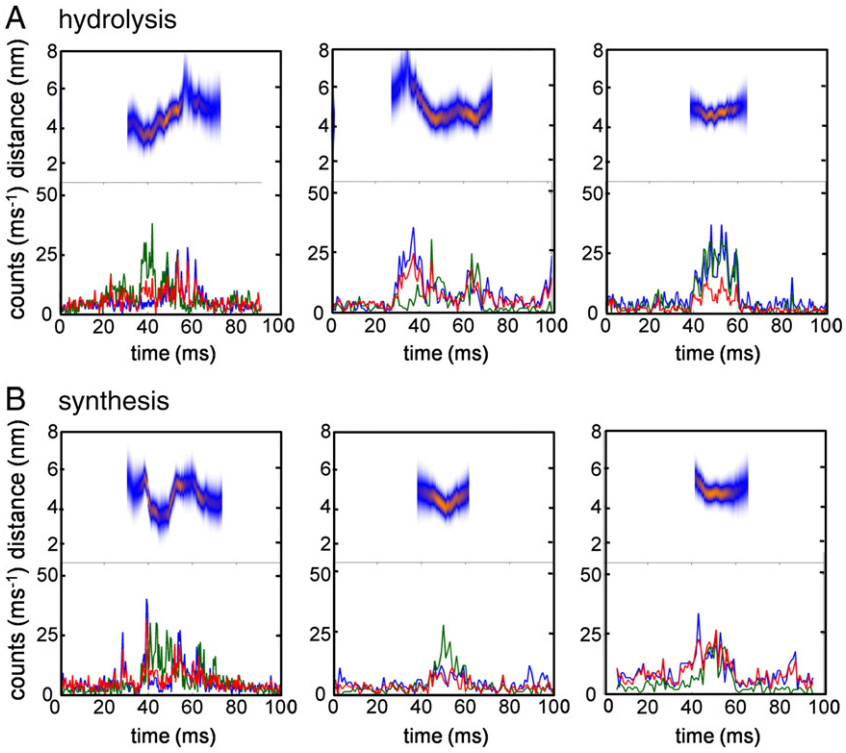

Fig. 3. Photon bursts of single FRET-labeled F_OF_1-ATP synthases during ATP hydrolysis (A, upper row) and ATP synthesis (B, lower row). Fluorescence intensity of the FRET donor Alexa-532 is shown as the blue trace in the lower panels and intensity of the FRET acceptor Cy5 as the green trace following 532 nm excitation. The presence of Cy5 on the enzyme was controlled by alternating laser excitation with 635 nm resulting in the simultaneous red trace of fluorescence. According to the Förster theory, corresponding distances between the fluorophores were calculated in the upper panels based on maximum likelihood estimations [56,58].

Table 1
Statistics of all FRET levels in photon bursts of single F_OF_1-ATP synthases during ATP hydrolysis.

	ATP hydrolysis 1 mM ATP	+1 mM AMPPNP	+60 μM DCCD
Number of photon bursts	556	225	164
FRET level	1191	307	208
Changing FRET levels 2 and more per burst	782 (65.7%)	71 (23.1%)	35 (16.8%)
Changing FRET levels 3 and more per burst	203 (36.5%)	21 (9.3%)	11 (6.7%)
FRET levels in sequential order	521	44	7
FRET levels in alternating order	146	12	20
Dwell time ± s.d.	7.8 ± 0.6 ms	18.8 ± 1.6 ms	23.6 ± 5.2 ms

Measurement times:

twenty 15-min measurements for ATP hydrolysis
ten 15-min measurements for AMPPNP or DCCD.

Fig. 3A (left and middle) exhibited fluctuations of FRET efficiencies, whereas a third enzyme (right panel) did not show FRET distance changes between the two fluorophores on the ε- and *c*-subunits.

Manually assigned FRET level and durations were stored in data files for further analysis. A total number of 1181 FRET levels were assigned in all photon bursts, that is, 782 levels in photon bursts with 2 and more FRET levels (~66% of all enzymes during ATP hydrolysis), or 203 levels in photon bursts with 3 and more FRET levels (~37% of all enzymes; see Table 1). For enzymes with 3 and more FRET levels the direction of FRET changes was discriminated. 521 FRET levels showed sequential changes, that is, stepwise increasing or decreasing distances between the two fluorophores. 146 FRET levels alternated corresponding to a back-and-forth movement, or a reversible twisting of the two rotor subunits. Photon bursts with 3 and more FRET levels were required also for the dwell time analysis of intermediary FRET levels, because the durations of the first and the last FRET levels remain unknown as the enzyme is diffusing in and out of the detection volume as described below.

The FRET dynamics in single F_OF_1-ATP synthases changed completely when the non-hydrolysable derivative AMPPNP was added (1 mM) instead of ATP to buffer A. Only 23% of the photon bursts showed 2 and more FRET levels, and the fraction of enzymes with 3 and more FRET levels was about 9% (Table 1). As found in the previous single-molecule FRET rotation studies with F_OF_1-ATP synthase, the presence of AMPPNP did not completely abolish rotor dynamics.

After addition of 60 μM DCCD to ATP hydrolysis buffer A with 1 mM ATP, the number of enzymes with FRET changes was reduced to a similar extent. Only 17% of photon bursts showed 2 and more FRET levels and ~7% showed 3 and more FRET levels, indicating that DCCD binding to the *c*-subunit blocks rotation in the F_O motor and likely stalls the elastic deformation of the rotor in the enzyme.

3.3. Single-molecule FRET recordings during ATP synthesis

To monitor elastic deformations during ATP synthesis, a 2-μl aliquot of reconstituted FRET-labeled F_OF_1-ATP synthase was thawed and diluted 5 times with an acidic buffer B (20 mM succinic acid–NaOH, 5 mM NaH_2PO_4, 100 μM ADP, 2.5 mM $MgCl_2$, 0.6 mM KOH, 20 μM valinomycin) at pH 4.7. After 2 min the acidified proteoliposomes were mixed 1:100 with basic buffer C (200 mM succinic acid, 5 mM NaH_2PO_4, 100 μM ADP, 2.5 mM $MgCl_2$, 160 mM KOH, adjusted to pH 8.8 with NaOH) generating a ΔpH of 4.1 and an K^+/valinomycin diffusion potential across the membrane as described for ATP synthesis measurements [60]. Immediately after mixing, 50 μl of the proteoliposomes was transferred as a droplet onto the microscope cover slip and single-molecule FRET trajectories were recorded. In Fig. 3B, three photon bursts of F_OF_1-ATP synthase are shown as sample data. The enzyme in the left panel showed large alternating fluctuations of the FRET efficiency, while the enzyme in the middle panel showed small transient FRET changes. However, some enzymes did not exhibit a distance change between the two fluorophores on the rotor for a significant period of time during ATP synthesis (right panel).

Photon burst statistics of assigned FRET levels during ATP synthesis are summarized in Table 2. A similar number of 478 FRET-labeled enzymes were recorded in twenty 10-min measurements, with a total number of 824 FRET levels. 64% of the photon bursts had 2 and more FRET levels, and 26% showed 3 and more FRET levels, with a 2:1 ratio for sequential FRET changes to alternating movements between the fluorophores.

3.4. Single-molecule FRET recordings in the presence of AMPPNP or DCCD during ATP synthesis conditions

Addition of 1 mM AMPPNP or 60 μM DCCD to the buffer C for FRET measurements during ATP synthesis caused a reduction in the fraction of enzymes showing fluctuations among 2 and more FRET levels to 16% or 13%, respectively, and in the fraction showing fluctuations among three or more FRET levels to7% and 2%, respectively. FRET-labeled F_OF_1-ATP synthases in the presence of 1 mM AMPPNP under ATP synthesis condition are shown in Fig. 4A and B. The enzyme in Fig. 4A underwent elastic deformation of the rotor, while the one in Fig. 4B remained unchanged with constant FRET efficiency over a long time. An example of a FRET-labeled enzyme in the presence of DCCD is shown in Fig. 4C, revealing a constant distance between the markers on the ε and one *c*-subunit. The distribution of FRET efficiencies in Fig. 4D covered the complete range of expected distances with equal probabilities, ranging from distances shorter than 5 nm (*i.e.* FRET efficiencies larger than 50 to 60%) to longer distances up to 7 nm (*i.e.* FRET efficiencies around 20 to 25%). However, this distribution was broadened due to the low photon numbers in single photon bursts. Similar FRET efficiency distributions were obtained for ATP hydrolysis condition in the absence and presence of DCCD.

3.5. Rotor twisting from FRET transition density plots

To identify the angular twisting as a transient elastic energy storage between the two rotor domains on the ε- and one *c*-subunit, we plotted all FRET level pairs from photon bursts with two and more FRET levels for enzymes working in ATP hydrolysis mode (Fig. 5A). The majority of FRET transitions were associated with small distance changes, that is, in the range of 0.6 to 0.8 nm. For example, several transitions were found

Table 2
Statistics of all FRET levels in photon bursts of single F_OF_1-ATP synthases during ATP synthesis.

	ATP synthesis 100 μM ADP	+1 mM AMPPNP	+60 μM DCCD
Number of photon bursts	478	89	41
FRET level	824	121	47
Changing FRET levels 2 and more per burst	527 (64.0%)	20 (16.5%)	6 (12.8%)
Changing FRET levels 3 and more per burst	125 (26.1%)	6 (6.7%)	1 (2.4%)
FRET levels in sequential order	304	60	1
FRET levels in alternating order	148	45	0
Dwell time ± s.d.	8.2 ± 0.9 ms	n.d.	n.d.

Measurement times:

twenty 10-min measurements for ATP synthesis
ten 10-min in the presence of AMPPNP or DCCD.

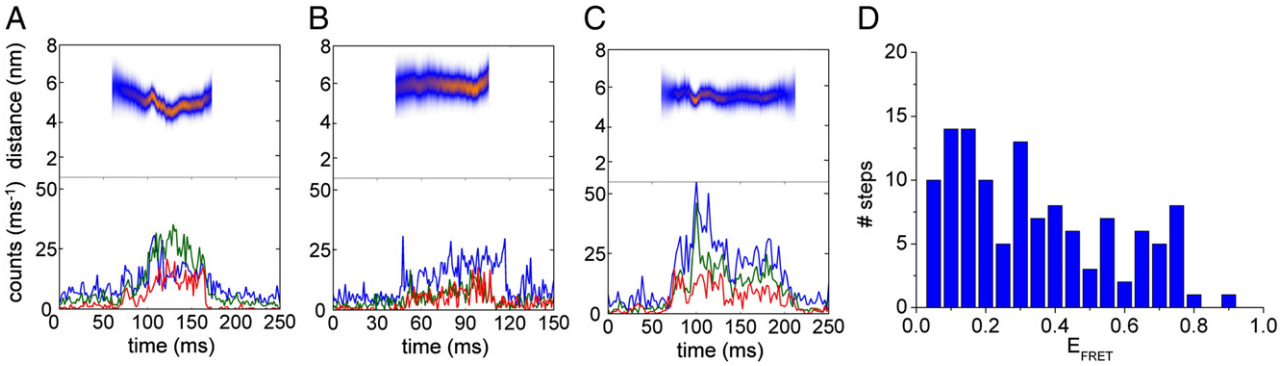

Fig. 4. Photon bursts of single FRET-labeled F_OF_1-ATP synthases during ATP synthesis in the presence of 1 mM AMPPNP (A, B) and 60 μM DCCD (C). Fluorescence intensity of the FRET donor Alexa-532 is shown as the blue trace in the lower panels and intensity of the FRET acceptor Cy5 as the green trace following 532 nm excitation. Distances between the fluorophores were calculated in the upper panels. The presence of Cy5 on the enzyme was controlled by alternating laser excitation with 635 nm resulting in the simultaneous red trace of fluorescence. (D) FRET efficiency histogram of single FRET-labeled F_OF_1-ATP synthases during ATP synthesis in the presence of 1 mM AMPPNP.

from 6.5 nm to 5.8 nm and *vice versa*. However, larger distance changes were detected as well. The distribution in this FRET transition density plot appeared to be symmetrical with respect to the diagonal. The small distance changes ($\Delta d_{1,2}$) from FRET level 1 to the next FRET level 2 were also obvious when we plotted the $\Delta d_{1,2}$ against each starting FRET level 1 (Fig. 5B).

To discriminate small sequential changes from alternating distance changes we applied a new FRET transition density plot based on pairs of subsequent distance changes (Fig. 5C). In the diagram, an increasing distance $\Delta d_{1,2}$ from the first to the second FRET level appeared in the right part at positive values of $\Delta d_{1,2}$, and a subsequent decrease in distance $\Delta d_{2,3}$ from the second to the third FRET level is found in the right lower at negative values of $\Delta d_{2,3}$. This frequently observed pattern could correspond to alternating movement of the labeled *c*-subunit with respect to ε. In the upper left part of the diagram, alternating distances appeared as well. In contrast, sequential FRET changes were allocated in the lower left or the upper right parts. During ATP hydrolysis, both types of distance changes were found, with a large fraction of alternating movements between ε and *c*.

Estimation of the extent of elastic deformation required geometric models for the observed FRET transitions. The models were developed according to Fig. 1B and the resulting constraints for the given stepwise twisting of the rotor in F_OF_1-ATP synthase were added as continuous ellipses into Fig. 5A–C. The thick black lines corresponded to deformations of a single 36° step of *c* for a given position of ε. A single 72° step or two fast and unresolved consecutive 36° steps corresponded to the dashed line, and a 108° twist of *c* is shown as the dotted black ellipse in Fig. 5.

The corresponding set of FRET transition density plots for ATP synthesis condition is shown as Fig. 5D, E, and F. FRET distance changes from one to the next FRET level were small (Fig. 5D) and in the range of maximum 1.5 nm. The majority of distance changes were less than 1 nm (Fig. 5E). From the subsequent distance change diagram (Fig. 5F), alternating FRET changes corresponding to larger back-and-forth fluctuations were dominant. However, a significant fraction of single 36° stepping of *c* with respect to ε cannot be ruled out, because the FRET distance change plots were hampered by the fact that distance changes near 0 nm cannot be assigned in the data, either by manual inspection or by computational threshold-based approaches.

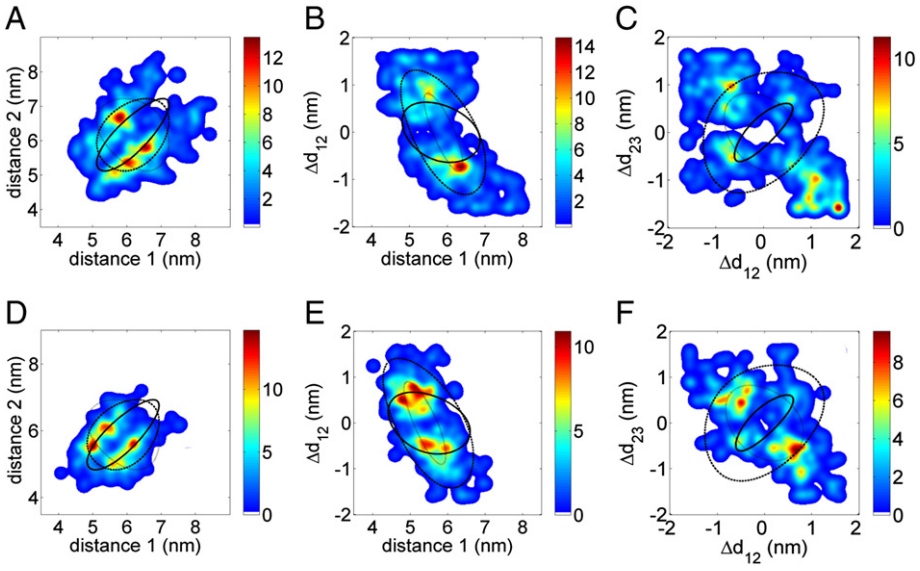

Fig. 5. FRET transition plots for consecutive FRET levels within a photon burst of single F_OF_1-ATP synthases during ATP hydrolysis (A–C) and ATP synthesis (D–F). The theoretical ellipses in the panels correspond to 36° twist (black solid lines), 72° twist (black dashed lines) and 108° (black dotted lines). A, D, FRET distance 1 to subsequent distance 2 plots for all assigned FRET level pairs. B, E, FRET distance change plots from distance 1 to larger or smaller distance 2. C, F, Plots of consecutive FRET distance changes observed in series of three and more FRET levels within a photon burst.

3.6. Simulations for FRET transitions

The simulated FRET transition plots for purely 36° steps for angular twisting of the rotor subunits ε and *c* as well as 72° steps and 108° steps are shown in Fig. 6. Here we assumed a ring diameter of 5.0 nm for the Cy5 label on the N-terminus of the *c*-subunit. The Alexa532 label on ε was placed to a position 2.0 nm away from the axis of rotation in the Monte Carlo simulations of ε-*versus*-*c* movements, and at a height of 5.5 nm above the ring of Cy5 positions. 5000 data points were computed for each relative movement of 36°, 72° and 108° twisting, and a sum intensity of 150 counts/ms at maximum was given. For each apparent FRET distance we added a distance error of 0.5 nm resulting in the blurred distributions seen in Fig. 6, which were comparable to the experimental data.

The objective of these simulations was to find the most significant way of plotting the FRET distance changes in order to discriminate the maximum angular twist within the rotor of F_OF_1-ATP synthase. Apparently, the simulated FRET transition density plots (Fig. 6A, D, G) were not distinctive enough. The theoretical ellipses are different for the three assumed twist angles, but once the FRET distance measurements have an error of 0.5 nm, the distributions become broadened and similar. Plotting FRET distance 1 *versus* the FRET distance change $\Delta d_{1,2}$ showed more pronounced differences (Fig. 6B, E H), however, they were still affected by the impossibility to assign very small distance changes of less than 0.5 nm in the experimental data. It was obvious from the simulations that the very small FRET distance changes appeared with high probability for the cases of ε-to-*c* orientations around the maximal or the minimal distances.

When we plotted the simulated pairs of subsequent FRET distance changes of $\Delta d_{1,2}$ *versus* $\Delta d_{2,3}$ the discrimination of 36° steps and 72° steps appeared to be less doubtful (Fig. 6C, F, I). A significant number of distance changes were found going from −1 nm to another −1 nm, or from +1 nm to +1 nm for 72° twist, which were not observed for 36°. For the larger twist of 108° the distance changes from +1 nm were followed by −1 nm, or from −1 nm by +1 nm. Thus it seemed to be possible to determine the maximum twist from the comparison of all three types of FRET transition plots.

3.7. Dwell times

Finally we analyzed the dwell times for the elastic deformations measured as FRET level changes. During ATP hydrolysis, fluctuations of the ε–*c* distance resulted in a mean dwell of 7.8 ms (Fig. 7A), which is significantly faster than the catalytic dwell of the 120° stepping ε-subunit (14 ± 3 ms [29]) or γ (19 ms [28]) and more comparable to the dwells of individual stepping *c*-subunits with respect to the non-rotating stator subunit *a* reported previously (13 ms [33]). For ATP synthesis, we found a similar mean dwell time of 8.2 ms (Fig. 7B) for the associated distance changes between the two markers on the rotor of F_OF_1-ATP synthase. Again, the dwell times were shorter than those for 120° stepping of ε (18 ± 6 ms [29]) or γ (51 ms [28]) and were in the range of individual stepping of the *c*-subunits (9 ± 1 ms [33]).

4. Discussion

The FRET-labeled F_OF_1-ATP synthase from *E. coli* with two fluorophores attached to the ε and *c*-subunits was functional for ATP hydrolysis and ATP synthesis after reconstitution in liposomes. The distances between the fluorophores fluctuated during catalysis between 5 and 7 nm in freely diffusing proteoliposomes traversing the confocal detection volume. Because we could not label a specific

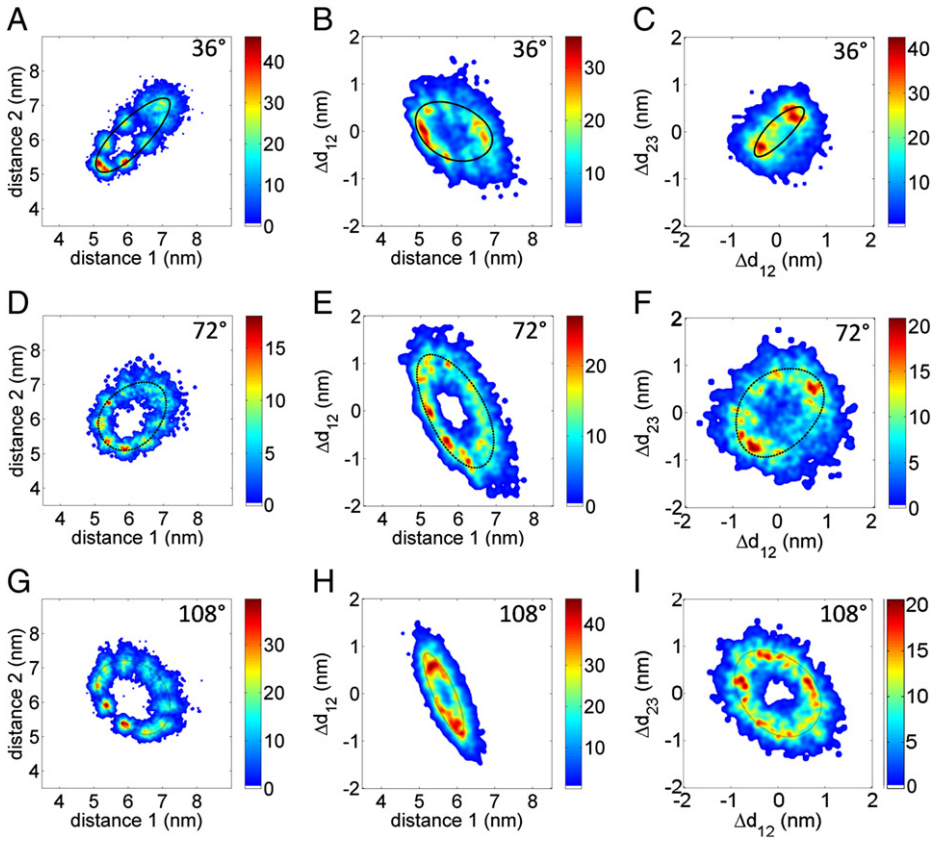

Fig. 6. Simulations of FRET transition plots based on Monte Carlo calculations for relative movements of *c*-subunits *versus* ε in steps of 36° (A, B, C), 72° (D, E, F) and 108° (G, H, I) for pattern comparison with the experimental distribution shown in Fig. 5. A FRET distance error of 0.5 nm was assumed and the FRET transition distributions were blurred.

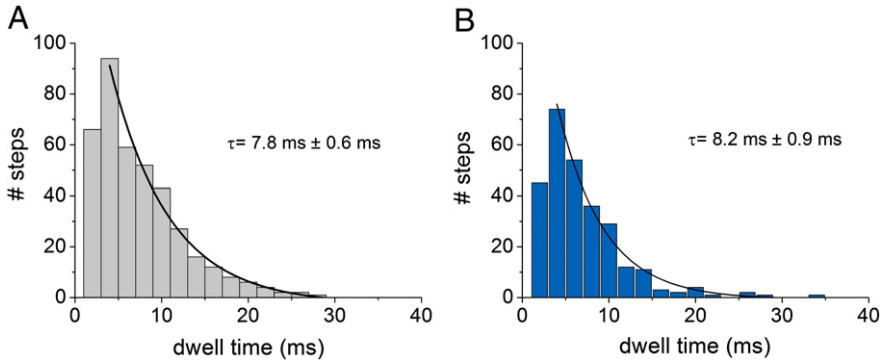

Fig. 7. Dwell time distributions of FRET levels in single F_OF_1-ATP synthases during ATP hydrolysis (A) and ATP synthesis (B). Dwell time binning was 2 ms. Histograms were fitted by a monoexponential decay function.

c-subunit with respect to the ε subunit, a maximum number of 10 possible FRET distances were expected. However, symmetry of the *c*-ring and the resolution limits of our FRET distance measurements in the range of 0.5 nm reduced the number of FRET distances that should be distinguished to about five. Given a Förster radius of 5.3 nm for the dye pair Alexa532–Cy5, the observed values of FRET distances were in the most sensitive region for this distance measurement method. Furthermore, we selected enzymes for further FRET analysis that exhibited fluorophore distances around the Förster radius by applying similar intensity thresholds for both FRET donor and acceptor photons of the burst.

Therefore we asked how far the rotor is twisted between the two domains labeled with the dyes, how fast the rotor is twisted, and if there are differences between ATP synthesis and ATP hydrolysis. To begin with the last question it seemed that the rotor is twisted in a similar way in both catalysis modes. The dwell times for stepwise changes in FRET levels were found in the range of 8 ms for each mode, and were comparable to the dwell time of *c*-ring rotation during ATP synthesis with respect to the stator subunit *a* of the enzyme [33]. These dwells were significantly faster than the previously reported dwell times of 14 to 51 ms for the 120° stepping of the ε and γ-subunits relative to the b_2 stator stalk for ATP hydrolysis and ATP synthesis. These shorter dwell times for the elastic deformation of the rotor would be expected for small twisting angles caused by *c*-subunit steps smaller than a single 120° step of *c versus* ε. Because fast *c*-ring steps within the F_O motor were associated with about 50% of single 36° steps of the *c*-subunit [33], the dwells for *c*–ε twisting here supported an one-after-another stepping mode of *c* before ε switched by 120° as conceived before [61].

In the presence of AMPPNP or 60 μM DCCD the number of intermediary FRET levels that could be used to build the dwell time histograms was so low (Tables 1 and 2) that we could hardly estimate a dwell time. However, the apparent dwell times were much longer indicating that the elastic deformation of the rotor is suppressed by these inhibitors. This was more obvious for ATP synthesis than for ATP hydrolysis. From the different ways of plotting FRET distances and subsequent distance changes applied here we conclude that a simple fluctuation mode with one given angle of 36° corresponding to a back-and-forth movement of the *c*-subunit with respect to ε cannot be inferred. Instead larger fluctuations of up to 108° seem to be the likely elastic distortion of the investigated rotor domains during catalysis based on the observed FRET distance changes of more than 1 nm. Simulations of rotor twisting FRET data using an increased signal-to-noise ratio resulted in a much better discrimination of the maximum twist in the FRET distance change plots provided in Figs. 5 and 6. Thus, refined FRET measurements would be useful and currently are in progress.

Alternative explanations for the observed FRET fluctuations have to be considered. For example, could a possible rotor axis bending during catalysis result in FRET distance variations? In previous single-molecule FRET measurements between the amino acid position ε56 and the static *b*-subunits we have found differences in the mean distance for the three stopping positions of ε. By single-molecule FRET triangulation these changes in the FRET histograms could be interpreted as being caused by a tilt in the rotor axis [29]. However, here we observed FRET fluctuations for the case of ATP hydrolysis and synthesis, but rarely for the inhibited rotation in the presence of AMPPNP or DCCD. If bending of the rotor axis in a back-and-forth manner should take place, we would not expect this to be found as FRET changes between the relatively rigid part of ε and the *c*-ring. The domain around position ε56, which was used for labeling, is considered to be tightly coupled to the *c*-ring especially during catalysis. Also stochastic relocations of the fluorophores between metastable positions in the local protein environments appear to be unlikely as a complete explanation, because we detected only a few apparent FRET fluctuations in the presence of AMPPNP or DCCD for similar photophysical conditions. The relatively poor photon statistics for the single-molecule FRET measurements still allowed demonstration of differences in stepping during catalysis and inhibited rotation in the presence of AMPPNP or DCCD. However, to solve the problem of an over-interpretation of the FRET data, several refinements of the measurements are required, for example using a microfluidic device for trapping the FRET-labeled enzymes as suggested below. At the moment, elastic deformation of the rotor seems to be a well-justified explanation of our FRET data.

Elasticity measurements of the rotor subunit have been reported previously with surface-attached F_1 sectors [10] and with F_OF_1-ATP synthases [43–45] in detergent. More than 40° of possible twisting was found within the γ/ε and *c*-subunits by observing the movement of large beads on the enzyme. In addition, the γ-subunit also has a smaller elastic component within the static $\alpha_3\beta_3$ subunits. Measurements of bead fluctuations attached to the rotor were followed by MD simulations to further identify the elastic portions of the rotor subunits on an atomic level [46]. Forced rotation and stalling of the rotor by magnetic beads, carefully controlled by external magnetic fields, yielded a high elasticity. In contrast, the full width at half maximum of the angular distribution of bead positions bound to the peripheral stator stalk in the range of less than 10° indicated a high stiffness of the right handed coiled-coil *b*-subunits in *E. coli* ATP synthase [39,45]. The single-molecule FRET data provided here indicate substantial twisting in the rotor, possibly approaching 108°, and strongly support the concept of elastic power transition in the rotary motors of F_OF_1-ATP synthase [36]. We were surprised that such extensive elasticity would be present in the protein structures located between the two fluorophores, *i.e.* the N-terminal β-barrel domain of ε and the *c*-ring. However, it should be noted that we detect only the dynamic FRET changes within a photon burst in our single-molecule FRET measurements. Therefore, the absolute twist during catalytic conditions and in the presence of AMPPNP could be even larger than

108° but a static twist angle cannot be identified in the photon burst because we have no *a priori* knowledge of which *c*-subunit was labeled with respect to ε56 and, accordingly, cannot deduce the twist angle in the single enzyme. Only dynamic FRET changes can be analyzed by our approach, in contrast to the surface-immobilized enzymes under different biochemical conditions discussed above.

By placing the fluorophores at other parts of the rotor [49] in the next series of FRET experiments, a complete map of domain elasticities could be obtained. It will be important to unravel whether torsional forces could twist the top of the *c*-ring (*i.e.* the polar loops where γ and ε bind) relative to the bottom, *i.e.* the periplasmic side. This changing of the crossing angles of the transmembrane helices of the *c*-subunits could provide another contribution to the soft spring of the rotor of F_OF_1-ATP synthase; so far, this potential elasticity has not been part of models for the F_O motor [17,62–64]. In addition, the elasticity provided by the region of γ between the base of $\alpha_3\beta_3$ and the β-barrel of ε should be explored.

For future experiments we need to solve the problems of limited time resolution and angular precision of the FRET approach. We likely missed substeps of twisting in those enzymes which showed large stepwise FRET distance changes. Because of the rapid dynamics we need to develop a different way of analyzing FRET photon statistics, for example correlation or cross-correlation of the two fluorescence time trajectories of FRET donor and acceptor [65]. These future FRET improvements will require fluorophores with higher quantum yields and optimized laser excitation in terms of wavelengths and duty cycle-optimized alternating excitation schemes [66]. Most importantly the observation time for a single proteoliposome has to be increased. This could be achieved by a method which compensates for the Brownian motion of the FRET-labeled enzyme. For example, an electrokinetic trap ('ABELtrap' developed by A E Cohen and W E Moerner) could be used to bring the FRET-labeled F_OF_1-ATP synthase into the laser focus and hold it there until the fluorophores photobleach, providing up to 10 s of continuous FRET measurements of a single enzyme molecule [67–70]. Finally, new ways to prove that the behavior of the enzyme measured *in vitro* also applies in the living cell have to be developed. Potentially, these will be based on the single-molecule analysis of subunit rotation and elastic deformation using very small, non-interfering markers and the Förster-type of resonance energy transfer.

Acknowledgements

We thank P. Gräber and coworkers (University of Freiburg) for their help in enzyme purification and J. Wrachtrup (University of Stuttgart) for supporting the development of the confocal setup. Financial support from the Deutsche Forschungsgemeinschaft (grant BO 1891/10-2 to M.B.), the Volkswagen Foundation (grant I/84073), and the Canadian Institutes of Health Research (grant MT-10237 to S.D.D.) is gratefully acknowledged.

References

[1] P.D. Boyer, The binding change mechanism for ATP synthase—some probabilities and possibilities, Biochim. Biophys. Acta 1140 (1993) 215–250.
[2] J.P. Abrahams, A.G. Leslie, R. Lutter, J.E. Walker, Structure at 2.8 A resolution of F1-ATPase from bovine heart mitochondria, Nature 370 (1994) 621–628.
[3] H. Noji, R. Yasuda, M. Yoshida, K. Kinosita Jr., Direct observation of the rotation of F1-ATPase, Nature 386 (1997) 299–302.
[4] R. Yasuda, H. Noji, M. Yoshida, K. Kinosita Jr., H. Itoh, Resolution of distinct rotational substeps by submillisecond kinetic analysis of F1-ATPase, Nature 410 (2001) 898–904.
[5] K. Adachi, K. Oiwa, T. Nishizaka, S. Furuike, H. Noji, H. Itoh, M. Yoshida, K. Kinosita Jr., Coupling of rotation and catalysis in F(1)-ATPase revealed by single-molecule imaging and manipulation, Cell 130 (2007) 309–321.
[6] R. Watanabe, R. Iino, H. Noji, Phosphate release in F1-ATPase catalytic cycle follows ADP release, Nat. Chem. Biol. 6 (2010) 814–820.
[7] Y. Rondelez, G. Tresset, T. Nakashima, Y. Kato-Yamada, H. Fujita, S. Takeuchi, H. Noji, Highly coupled ATP synthesis by F1-ATPase single molecules, Nature 433 (2005) 773–777.
[8] H. Itoh, A. Takahashi, K. Adachi, H. Noji, R. Yasuda, M. Yoshida, K. Kinosita, Mechanically driven ATP synthesis by F1-ATPase, Nature 427 (2004) 465–468.
[9] R. Watanabe, D. Okuno, S. Sakakihara, K. Shimabukuro, R. Iino, M. Yoshida, H. Noji, Mechanical modulation of catalytic power on F(1)-ATPase, Nat. Chem. Biol. 8 (2012) 86–92.
[10] D. Okuno, R. Iino, H. Noji, Stiffness of gamma subunit of F(1)-ATPase, Eur. Biophys. J. 39 (2010) 1589–1596.
[11] Y. Kato-Yamada, H. Noji, R. Yasuda, K. Kinosita Jr., M. Yoshida, Direct observation of the rotation of epsilon subunit in F1-ATPase, J. Biol. Chem. 273 (1998) 19375–19377.
[12] K. Hasler, S. Engelbrecht, W. Junge, Three-stepped rotation of subunits gamma and epsilon in single molecules of F-ATPase as revealed by polarized, confocal fluorometry, FEBS Lett. 426 (1998) 301–304.
[13] M. Nakanishi-Matsui, S. Kashiwagi, H. Hosokawa, D.J. Cipriano, S.D. Dunn, Y. Wada, M. Futai, Stochastic high-speed rotation of *Escherichia coli* ATP synthase F1 sector: the epsilon subunit-sensitive rotation, J. Biol. Chem. 281 (2006) 4126–4131.
[14] Y. Sambongi, Y. Iko, M. Tanabe, H. Omote, A. Iwamoto-Kihara, I. Ueda, T. Yanagida, Y. Wada, M. Futai, Mechanical rotation of the c subunit oligomer in ATP synthase (F0F1): direct observation, Science (New York, N.Y.) 286 (1999) 1722–1724.
[15] O. Panke, K. Gumbiowski, W. Junge, S. Engelbrecht, F-ATPase: specific observation of the rotating c subunit oligomer of EF(o)EF(1), FEBS Lett. 472 (2000) 34–38.
[16] H. Ueno, T. Suzuki, K. Kinosita Jr., M. Yoshida, ATP-driven stepwise rotation of FoF1-ATP synthase, Proc. Natl. Acad. Sci. U. S. A. 102 (2005) 1333–1338.
[17] R. Ishmukhametov, T. Hornung, D. Spetzler, W.D. Frasch, Direct observation of stepped proteolipid ring rotation in *E. coli* FF-ATP synthase, EMBO J. 29 (2010) 3911–3923.
[18] R. Iino, K.C. Tham, K.V. Tabata, H. Ueno, H. Noji, Direct observation of steps in c-ring rotation of *Escherichia coli* F(0)F(1)-ATP synthase, Biochim. Biophys. Acta-Bioenerg. 1797 (2010) 34 (Supplement).
[19] T.M. Duncan, V.V. Bulygin, Y. Zhou, M.L. Hutcheon, R.L. Cross, Rotation of subunits during catalysis by *Escherichia coli* F1-ATPase, Proc. Natl. Acad. Sci. U. S. A. 92 (1995) 10964–10968.
[20] Y. Zhou, T.M. Duncan, R.L. Cross, Subunit rotation in *Escherichia coli* FoF1-ATP synthase during oxidative phosphorylation, Proc. Natl. Acad. Sci. U. S. A. 94 (1997) 10583–10587.
[21] G. Kaim, M. Prummer, B. Sick, G. Zumofen, A. Renn, U.P. Wild, P. Dimroth, Coupled rotation within single F0F1 enzyme complexes during ATP synthesis or hydrolysis, FEBS Lett. 525 (2002) 156–163.
[22] S.P. Tsunoda, R. Aggeler, M. Yoshida, R.A. Capaldi, Rotation of the c subunit oligomer in fully functional F1Fo ATP synthase, Proc. Natl. Acad. Sci. U. S. A. 98 (2001) 898–902.
[23] M. Borsch, M. Diez, B. Zimmermann, R. Reuter, P. Graber, Monitoring gamma-subunit movement in reconstituted single EFoF1 ATP synthase by fluorescence resonance energy transfer, in: R. Kraayenhof, A.J.W. Visser, H.C. Gerritsen (Eds.), Fluorescence spectroscopy, Imaging and Probes. New Tools in Chemical, Physical and Life Sciences, vol. 2, Springer-Verlag, Berlin, 2002, pp. 197–207.
[24] M. Borsch, M. Diez, B. Zimmermann, M. Trost, S. Steigmiller, P. Graber, Stepwise rotation of the gamma-subunit of EFoF1-ATP synthase during ATP synthesis: a single-molecule FRET approach, Proc. SPIE 4962 (2003) 11–21.
[25] S. Steigmiller, B. Zimmermann, M. Diez, M. Borsch, P. Graber, Binding of single nucleotides to H+-ATP synthases observed by fluorescence resonance energy transfer, Bioelectrochemistry 63 (2004) 79–85.
[26] R. Bienert, V. Rombach-Riegraf, M. Diez, P. Graber, Subunit movements in single membrane-bound H+-ATP synthases from chloroplasts during ATP synthesis, J. Biol. Chem. 284 (2009) 36240–36247.
[27] M. Borsch, M. Diez, B. Zimmermann, R. Reuter, P. Graber, Stepwise rotation of the gamma-subunit of EF(0)F(1)-ATP synthase observed by intramolecular single-molecule fluorescence resonance energy transfer, FEBS Lett. 527 (2002) 147–152.
[28] M. Diez, B. Zimmermann, M. Borsch, M. Konig, E. Schweinberger, S. Steigmiller, R. Reuter, S. Felekyan, V. Kudryavtsev, C.A. Seidel, P. Graber, Proton-powered subunit rotation in single membrane-bound F0F1-ATP synthase, Nat. Struct. Mol. Biol. 11 (2004) 135–141.
[29] B. Zimmermann, M. Diez, N. Zarrabi, P. Graber, M. Borsch, Movements of the epsilon-subunit during catalysis and activation in single membrane-bound H(+)-ATP synthase, EMBO J. 24 (2005) 2053–2063.
[30] M.G. Duser, Y. Bi, N. Zarrabi, S.D. Dunn, M. Borsch, The proton-translocating a subunit of F_0F_1-ATP synthase is allocated asymmetrically to the peripheral stalk, J. Biol. Chem. 283 (2008) 33602–33610.
[31] B. Zimmermann, M. Diez, M. Borsch, P. Graber, Subunit movements in membrane-integrated EF_0F_1 during ATP synthesis detected by single-molecule spectroscopy, Biochim. Biophys. Acta 1757 (2006) 311–319.
[32] K.M. Johnson, L. Swenson, A.W. Opipari Jr., R. Reuter, N. Zarrabi, C.A. Fierke, M. Borsch, G.D. Glick, Mechanistic basis for differential inhibition of the F(1)F(o)-ATPase by aurovertin, Biopolymers 91 (2009) 830–840.
[33] M.G. Duser, N. Zarrabi, D.J. Cipriano, S. Ernst, G.D. Glick, S.D. Dunn, M. Borsch, 36 degrees step size of proton-driven c-ring rotation in FoF1-ATP synthase, EMBO J. 28 (2009) 2689–2696.
[34] H. Imamura, M. Nakano, H. Noji, E. Muneyuki, S. Ohkuma, M. Yoshida, K. Yokoyama, Evidence for rotation of V1-ATPase, Proc. Natl. Acad. Sci. U. S. A. 100 (2003) 2312–2315.
[35] S. Furuike, M. Nakano, K. Adachi, H. Noji, K. Kinosita Jr., K. Yokoyama, Resolving stepping rotation in *Thermus thermophilus* H(+)-ATPase/synthase with an essentially drag-free probe, Nat. Commun. 2 (2011) 233.
[36] D.A. Cherepanov, A.Y. Mulkidjanian, W. Junge, Transient accumulation of elastic energy in proton translocating ATP synthase, FEBS Lett. 449 (1999) 1–6.

[37] O. Panke, B. Rumberg, Kinetic modeling of rotary CF0F1-ATP synthase: storage of elastic energy during energy transduction, Biochim. Biophys. Acta 1412 (1999) 118–128.
[38] W. Junge, O. Panke, D.A. Cherepanov, K. Gumbiowski, M. Muller, S. Engelbrecht, Inter-subunit rotation and elastic power transmission in F0F1-ATPase, FEBS Lett. 504 (2001) 152–160.
[39] P.A. Del Rizzo, Y. Bi, S.D. Dunn, ATP synthase b subunit dimerization domain: a right-handed coiled coil with offset helices, J. Mol. Biol. 364 (2006) 735–746.
[40] S.B. Claggett, M. O'Neil Plancher, S.D. Dunn, B.D. Cain, The b subunits in the peripheral stalk of F1F0 ATP synthase preferentially adopt an offset relationship, J. Biol. Chem. 284 (2009) 16531–16540.
[41] S. Steigmiller, M. Borsch, P. Graber, M. Huber, Distances between the b-subunits in the tether domain of F(0)F(1)-ATP synthase from *E. coli*, Biochim. Biophys. Acta 1708 (2005) 143–153.
[42] O. Panke, D.A. Cherepanov, K. Gumbiowski, S. Engelbrecht, W. Junge, Viscoelastic dynamics of actin filaments coupled to rotary F-ATPase: angular torque profile of the enzyme, Biophys. J. 81 (2001) 1220–1233.
[43] H. Sielaff, H. Rennekamp, A. Wachter, H. Xie, F. Hilbers, K. Feldbauer, S.D. Dunn, S. Engelbrecht, W. Junge, Domain compliance and elastic power transmission in rotary F(O)F(1)-ATPase, Proc. Natl. Acad. Sci. U. S. A. 105 (2008) 17760–17765.
[44] W. Junge, H. Sielaff, S. Engelbrecht, Torque generation and elastic power transmission in the rotary FOF1-ATPase, Nature 459 (2009) 364–370.
[45] A. Wachter, Y. Bi, S.D. Dunn, B.D. Cain, H. Sielaff, F. Wintermann, S. Engelbrecht, W. Junge, Two rotary motors in F-ATP synthase are elastically coupled by a flexible rotor and a stiff stator stalk, Proc. Natl. Acad. Sci. U. S. A. 108 (2011) 3924–3929.
[46] J. Czub, H. Grubmuller, Torsional elasticity and energetics of F1-ATPase, Proc. Natl. Acad. Sci. U. S. A. 108 (2011) 7408–7413.
[47] N. Zarrabi, S. Ernst, M.G. Duser, A. Golovina-Leiker, W. Becker, R. Erdmann, S.D. Dunn, M. Borsch, Simultaneous monitoring of the two coupled motors of a single FoF1-ATP synthase by three-color FRET using duty cycle-optimized triple-ALEX, Proc. SPIE 7185 (2009) 718505.
[48] S. Ernst, M.G. Düser, N. Zarrabi, M. Börsch, Three-color Förster resonance energy transfer within single FOF1-ATP synthases: monitoring elastic deformations of the rotary double motor in real time, J. Biomed. Opt. J. Biomed. Opt. 17 (2012) 011004.
[49] V. Rombach-Riegraf, J. Petersen, E. Galvez, P. Gräber, S1.19 Observation of rotation of subunit c in the membrane integrated EF0F1 by single molecule fluorescence, Biochim. Biophys. Acta (BBA) - Bioenerg. 1777 (2008) S13 Supplement.
[50] S. Fischer, P. Graber, Comparison of DeltapH- and Delta***φ;***-driven ATP synthesis catalyzed by the H(+)-ATPases from *Escherichia coli* or chloroplasts reconstituted into liposomes, FEBS Lett. 457 (1999) 327–332.
[51] S. Ernst, C. Batisse, N. Zarrabi, B. Bottcher, M. Borsch, Regulatory assembly of the vacuolar proton pump VoV1-ATPase in yeast cells by FLIM-FRET, Proc. SPIE 7569 (2010) 75690W.
[52] F.E. Alemdaroglu, S.C. Alexander, D.M. Ji, D.K. Prusty, M. Borsch, A. Herrmann, Poly(BODIPY)s: a New class of tunable polymeric dyes, Macromolecules 42 (2009) 6529–6536.
[53] B. Verhalen, S. Ernst, M. Borsch, S. Wilkens, Dynamic ligand induced conformational rearrangements in P-glycoprotein as probed by fluorescence resonance energy transfer spectroscopy, J. Biol. Chem. 287 (2012) 1112–1127.
[54] S. Ernst, A.K. Schonbauer, G. Bar, M. Borsch, A. Kuhn, YidC-driven membrane insertion of single fluorescent Pf3 coat proteins, J. Mol. Biol. 412 (2011) 165–175.
[55] A.N. Kapanidis, N.K. Lee, T.A. Laurence, S. Doose, E. Margeat, S. Weiss, Fluorescence-aided molecule sorting: analysis of structure and interactions by alternating-laser excitation of single molecules, Proc. Natl. Acad. Sci. U. S. A. 101 (2004) 8936–8941.
[56] N. Zarrabi, M.G. Duser, S. Ernst, R. Reuter, G.D. Glick, S.D. Dunn, J. Wrachtrup, M. Borsch, Monitoring the rotary motors of single FoF1-ATP synthase by synchronized multi channel TCSPC, Proc. SPIE 6771 (2007) 67710F.
[57] N. Zarrabi, B. Zimmermann, M. Diez, P. Graber, J. Wrachtrup, M. Borsch, Asymmetry of rotational catalysis of single membrane-bound F0F1-ATP synthase, Proc. SPIE 5699 (2005) 175–188.
[58] G.F. Schroder, H. Grubmuller, Maximum likelihood trajectories from single molecule fluorescence resonance energy transfer experiments, J. Chem. Phys. 119 (2003) 9920–9924.
[59] T. Forster, Energiewanderung Und Fluoreszenz, Naturwissenschaften 33 (1946) 166–175.
[60] S. Steigmiller, P. Turina, P. Graber, The thermodynamic H+/ATP ratios of the H+-ATP synthases from chloroplasts and *Escherichia coli*, Proc. Natl. Acad. Sci. U. S. A. 105 (2008) 3745–3750.
[61] W. Junge, H. Lill, S. Engelbrecht, ATP synthase: an electrochemical transducer with rotatory mechanics, Trends Biochem. Sci. 22 (1997) 420–423.
[62] S.B. Vik, B.J. Antonio, A mechanism of proton translocation by F1F0 ATP synthases suggested by double mutants of the a subunit, J. Biol. Chem. 269 (1994) 30364–30369.
[63] T. Elston, H. Wang, G. Oster, Energy transduction in ATP synthase, Nature 391 (1998) 510–513.
[64] A. Aksimentiev, I.A. Balabin, R.H. Fillingame, K. Schulten, Insights into the molecular mechanism of rotation in the F-o sector of ATP synthase, Biophys. J. 86 (2004) 1332–1344.
[65] T. Torres, M. Levitus, Measuring conformational dynamics: a new FCS-FRET approach, J. Phys. Chem. 111 (2007) 7392–7400.
[66] M. Borsch, J. Wrachtrup, Improving FRET-based monitoring of single chemomechanical rotary motors at work, Chemphyschem 12 (2011) 542–553.
[67] A.E. Cohen, W.E. Moerner, The anti-Brownian electrophoretic trap (ABEL trap): fabrication and software, Proc. SPIE 5699 (2005) 296–305.
[68] A.E. Cohen, W.E. Moerner, Suppressing Brownian motion of individual biomolecules in solution, Proc. Natl. Acad. Sci. U. S. A. 103 (2006) 4362–4365.
[69] R.H. Goldsmith, W.E. Moerner, Watching conformational- and photodynamics of single fluorescent proteins in solution, Nat. Chem. 2 (2010) 179–186.
[70] M. Borsch, Single-molecule fluorescence resonance energy transfer techniques on rotary ATP synthases, Biol. Chem. 392 (2011) 135–142.